Dynamic protein composition of Arabidopsis thaliana cytosolic ribosomes in response to sucrose feeding as revealed by label free MSE proteomics

ARTICLE *in* PROTEOMICS · APRIL 2012

Impact Factor: 3.81 · DOI: 10.1002/pmic.201100413 · Source: PubMed

6 AUTHORS, INCLUDING:

Maureen Hummel
University of California, Riverside
7 PUBLICATIONS **137** CITATIONS
SEE PROFILE

Jan Cordewener
Wageningen University
66 PUBLICATIONS **1,084** CITATIONS
SEE PROFILE

Antoine H.P. America
Wageningen University
59 PUBLICATIONS **1,426** CITATIONS
SEE PROFILE

DOI 10.1002/pmic.201100413 *Proteomics* 2012, *12*, 1024–1038

RESEARCH ARTICLE

Dynamic protein composition of *Arabidopsis thaliana* cytosolic ribosomes in response to sucrose feeding as revealed by label free MS^E proteomics

Maureen Hummel[1*], *Jan H. G. Cordewener*[2], *Joost C. M. de Groot*[2**], *Sjef Smeekens*[1,3], *Antoine H. P. America*[2,3,4] *and Johannes Hanson*[1,3,5]

[1] Molecular Plant Physiology, Utrecht University, Utrecht, The Netherlands
[2] BU Bioscience, Plant Research International, Wageningen, The Netherlands
[3] Centre for BioSystems Genomics, Wageningen, The Netherlands
[4] Netherlands Proteomics Centre, Utrecht, The Netherlands
[5] Umeå Plant Science Center, Department of Plant Physiology, Umeå University, Umeå, Sweden

Received: August 12, 2011
Revised: December 21, 2011
Accepted: January 17, 2012

Cytosolic ribosomes are among the largest multisubunit cellular complexes. *Arabidopsis thaliana* ribosomes consist of 79 different ribosomal proteins (r-proteins) that each are encoded by two to six (paralogous) genes. It is unknown whether the paralogs are incorporated into the ribosome and whether the relative incorporation of r-protein paralogs varies in response to environmental cues. Immunopurified ribosomes were isolated from *A. thaliana* rosette leaves fed with sucrose. Trypsin digested samples were analyzed by qTOF-LC-MS using both MS^E and classical MS/MS. Peptide features obtained by using these two methods were identified using MASCOT and Proteinlynx Global Server searching the theoretical sequences of *A. thaliana* proteins. The *A. thaliana* genome encodes 237 r-proteins and 69% of these were identified with proteotypic peptides for most of the identified proteins. These r-proteins were identified with average protein sequence coverage of 32% observed by MS^E. Interestingly, the analysis shows that the abundance of r-protein paralogs in the ribosome changes in response to sucrose feeding. This is particularly evident for paralogous RPS3aA, RPS5A, RPL8B, and RACK1 proteins. These results show that protein synthesis in the *A. thaliana* cytosol involves a heterogeneous ribosomal population. The implications of these findings in the regulation of translation are discussed.

Keywords:
Arabidopsis thaliana / Heterogeneity / Label-free LC-MS^E / Paralogs / Plant proteomics / Ribosomes

1 Introduction

Ribosome biogenesis and mRNA translation are highly energy demanding cellular processes. Ribosome biogenesis in the yeast *Saccharomyces cerevisiae* accounts for about 60% of all nuclear gene transcription, reviewed in [1]. Limiting energy supply restricts translational capacity, cell growth, and differentiation. Low energy levels trigger cells to switch to an energy preservation mode to maintain essential cell

Correspondence: Dr. Johannes Hanson, Molecular Plant Physiology, Utrecht University, Padualaan 8, 3584 CH, Utrecht, The Netherlands
E-mail: s.j.hanson@uu.nl
Fax: +31-30-253-3655

Abbreviations: BH, Benjamini-Hochberg; **DDA**, data-dependent acquisition; **DIA**, data-independent acquisition; **MAD**, median absolute deviation; **MS^E**, alternating acquisition of low and high collision energy mass spectrometry; **PLGS**, Proteinlynx Global Server; **RPL**, ribosome protein large subunit; **r-protein**, ribosomal protein; **RPP**, ribosome acidic phosphoprotein; **RPS**, ribosome protein small subunit; **TAIR**, The Arabidopsis Information Resource

*Present address: Maureen Hummel, Center for Plant Cell Biology, Department of Botany and Plant Sciences, University of California, Riverside, CA 92521-0124, USA
**Deceased 11.11.2010.

functions and viability, which results in inhibition of ribosome biogenesis, reviewed in [2]. This response is well conserved and is found in most, if not all eukaryotes, including plants. Stress factors change the expression of plant ribosomal protein (r-protein) and ribosomal biogenesis genes and thereby affect ribosomal biogenesis. Extended night or shading results in low sugar levels, which affect ribosome gene expression, while added sugar antagonizes the extended night responses [3–6].

Ribosomes are large ribonucleoprotein complexes composed of many different r-proteins, several rRNAs, and associated proteins. Eukaryotic 80S cytosolic ribosomes have been described in detail for yeast (*S. cerevisiae*), rat (*Rattus norvegicus*), wheat, and humans (*Homo sapiens*). These studies show that the ribosome contains four distinct rRNAs, the 18S rRNA of the 40S small ribosomal subunit and 5, 5.8, and 23S rRNAs of the 60S large ribosomal subunit. In addition, about 80 distinct r-proteins are present in the ribosome, depending on species. The exact localization of individual r-proteins in the ribosome remained unclear until crystal structures of bacterial and archaeal subunits at atomic resolution became available [7, 8]. These publications and others on the structures of prokaryotic ribosomes shed light on structural aspects of protein translation by ribosomes reviewed in [9]. Recent structures of eukaryotic cytoplasmic ribosomes have confirmed the similarities as well as differences between eukaryotic 80S and prokaryotic 70S ribosomes [10–12]. MS analysis of cytosolic ribosomes of rat, yeast, and humans provided insight in ribosomal composition and posttranslation modifications of ribosomes [13–17]. For example, phosphorylation and methylation modifications of RPL13a (ribosome protein large subunit 13a) and RPS2 (ribosome protein small subunit 2) have been linked to changes in ribosomal function and biogenesis, respectively [18, 19].

The composition of 80S cytosolic ribosomes of plants has been reported [20–25]. In *Arabidopsis thaliana* and maize (*Zea mays* L.) ribosomal covalent modifications are highly conserved when compared to the covalent modifications in yeast and mammals [20, 21, 24, 26]. Analysis of expressed sequence tags and the *A. thaliana* genome sequence have identified 251 r-protein genes, including 21 pseudogenes. These 251 r-protein genes encode 79 different types of r-proteins (31 small subunit proteins, RPS, and 48 large subunit proteins, RPL/RPP (ribosome acidic phosphoprotein)), numbers comparable to other eukaryotes. Recently, the identification by MS of 78 of the 79 *A. thaliana* cytosolic r-protein types was reported in ribosome complexes [22, 24, 25]. Mammalian r-proteins are encoded by single genes [27] but in *A. thaliana* each r-protein is encoded by multiple expressed genes (two to six) that form a small r-protein gene family. Such r-protein gene redundancy is also observed in rice (*Oryza sativa*) and to a lesser extent in the yeast *S. cerevisiae* [15, 28]. Most r-proteins are conserved between *A. thaliana* and mammals, with the exception of the plant specific P3 acidic phosphoprotein (RPP3) of the P1/P2 family [21, 29].

Public EST data and microarray hybridization results show that most plant r-protein family member genes are expressed. The expression patterns of plant r-protein genes are generally similar, in accordance with coexpression of r-protein genes in other organisms. However, striking deviations from the coexpression patterns are evident. This suggests that different r-protein family members might be present in the ribosome population at different points of development, in different cell types or during different growth conditions [30]. The biological function of ribosome heterogeneity is at present unclear. Studies performed on *A. thaliana* and maize ribosomes so far [21, 22, 24–26] have identified different r-protein paralogs within ribosomes, showing the heterogeneous nature of plant ribosomes. Genetic analysis has shown that individual *A. thaliana* genes encoding r-protein paralogs can be mutated without major effects on translation and that these genes in several cases have differential functionality, reviewed in [31], and for yeast in [32]. These studies further indicate concurrent expression of r-protein paralogs and ribosome heterogeneity in yeast and plant ribosomes but do not provide quantitative data of r-proteins nor insight in r-protein dynamics. Here, we identify and quantify *A. thaliana* r-proteins using label-free quantitative proteomics. Ribosomes were immunopurified from *A. thaliana* plants expressing His-FLAG-tagged ribosome protein RPL18B. This isolation procedure has previously been shown to efficiently purify actively translating ribosomes [33, 34]. Here, the riboproteomes of sucrose- versus control-treated rosette leaves have been determined. Sucrose was previously shown to inhibit translation of the bZIP11 transcription factor via a translational stalling mechanism involving an upstream open reading frame [35]. bZIP11 is a member of the S1 group bZIP transcription factors that appear to be important regulators of metabolism [36, 37]. All S1 group members are similarly translationally regulated in the same way by sucrose [38]. Tryptic digests of ribosomal extracts were analyzed by nanoUPLC-QTOF in MS^E mode and peptide/peak intensity data were processed by appropriate software packages. Multivariate analysis by principal component analysis (PCA) after normalization demonstrated the separation of the sucrose-treated and nontreated material. Database searching of the peptide fragmentation data resulted in identification of the majority (69%) of the expected 237 r-proteins with paralog-specific resolution for most of the identified proteins. This is the first quantitative assessment of the plant cytosolic riboproteome and its adjustment to changing growth conditions.

2 Material and methods

2.1 Plant materials and growth conditions

Transgenic 35S:HF-RPL18 [33] plants were grown on soil in long day conditions (16 h light/8 h dark) under cool white fluorescent light (150 μmol m^{-2} sec^{-1}) at 22°C, 70% relative

humidity. Rosette leaves of 4- to 5-wk-old plants were harvested from three independent batches of plants (Supporting Information Fig. S1) and incubated for 24 h in a Microclima cabinet (Snijders, Tilburg, The Netherlands) on a rotary shaker (60 rpm) under constant white fluorescent light (100 μE m^{-2}) in liquid 0.5 × Murashige-Skoog media (Duchefa, Haarlem, The Netherlands), pH 5.8 supplemented with 0.5 g/L 1,2-(N-morpholino) ethanesulfonic acid with or without the addition of 6% sucrose (w/v). Leaf material was snap frozen in liquid nitrogen, pulverized, and stored at −80°C prior to immunopurification.

2.2 Immunopurification of ribosomes

Ribosomes were isolated twice from each isolate of transgenic *A. thaliana* rosette leaves (Supporting Information Fig. S1) according to Zanetti et al. [33] with minor modifications. Frozen, pulverized leaf tissue was homogenized with two volumes of polysome extraction buffer (PEB). Homogenates were clarified by centrifugation at 16 000 × *g* for 10 min, and approximately 300 OD_{600} units of the supernatant were incubated with approximately 200 μL ANTI-FLAG® M2 Affinity Gel beads (Sigma, St. Louis, MA, USA) at 4°C for 2 h with gentle rotation. The supernatant fraction was recovered, and the beads were rapidly rinsed and then washed for 5 min with 4-mL PEB per 200-μL ANTI-FLAG® M2 Affinity Gel beads, followed by a 5 min wash with 4-mL wash buffer (100 mM Tris-HCl, pH 8.5, 200 mM KCl, 25 mM EGTA, 36 mM $MgCl_2$, 5 mM DTT, 1 mM PMSF, 50 μg/mL cycloheximide, 50 μg/mL chloramphenicol and 50 U/mL RNase inhibitor (Fermentas, Leon-Rot, Germany) per 200-μL ANTI-FLAG® M2 Affinity Gel beads. Elution was performed by incubation of the agarose beads with 400 μL of wash buffer containing 200 ng/μL of 3X FLAG® Peptide (Sigma) at 4°C for 30 min. Aliquots of eluted material were stored at −80°C prior to gel analysis or trypsin digestion and MS analysis.

2.3 SDS-PAGE and Western blotting

Proteins were separated on 15% (w/v) SDS-PAGE and stained with Coomassie Blue R250, silver staining plus (Bio-Rad, Hercules, CA, USA) or subjected to immunoblot analyses. Protein was precipitated using four volumes acetone and the precipitate was dissolved in 2× Laemmli loading buffer. Protein was loaded to 15% SDS-PAGE and electrophoresed using a Mini-Protean II system (Bio-Rad). Proteins were transferred to PVDF Western blotting membranes (Roche, Basel, Switzerland) according to standard procedures [39]. For immunological detection of FLAG-His-RPL18 or cFBPase, membranes were blocked for 1 h in PBST (1 mM Na_2HPO_4, 0.14 mM KH_2PO_4, 13.7 mM NaCl, 0.27 mM KCl, and 0.1% [v/v] Tween 20) that contained 3% (w/v) fat-free milk powder and were incubated for 1 h in PBST containing 3% fat-free milk powder with a 1:1000 dilution of mouse Monoclonal ANTI-FLAG® M2 antibody (Sigma) or 1:10 000 dilution of polyclonal anti-cFBPase (Agrisera, Vännäs, Sweden). Blots were washed three times in PBST and were incubated in PBST that contained 3% (w/v) fat-free milk powder with a 1:5 000 dilution of bovine antimouse IgG HRP conjugate (Santa Cruz Biotechnology, Santa Cruz, USA) or 1:8000 dilution of goat antirabbit IgG HRP conjugate (Santa Cruz Biotechnology) for 1 h. Blots were further washed four times in PBST and the antibody-antigen interaction was detected by adding 100 volumes luminol solution (100 mM Tris-HCl pH 8.6, 0.025% (w/v) luminol (Sigma) and 0.01% (v/v) H_2O_2) and one volume enhancer solution (0.11% para-hydroxycoumaric acid in 10-mL DMSO) to the blot and exposed to Kodak Biomax films (Sigma).

2.4 Trypsin digestion and peptide purification

Affinity purified polysomes (100 μL) were precipitated by addition of eight volumes of cold acetone and incubated at −20°C for at least 1 h. After centrifugation, the pellet was washed with 80% acetone and dried in air. The pellet was resuspended in 50 μL 0.1% (w/v) RapiGest SF Surfactant (Waters, Milford, MA, USA), 5 mM DTT (Sigma) in 0.1 M ammonium bicarbonate and incubated at 60°C for 1 h. Alkylation was performed by incubation with 15 mM iodoacetamide (IAA) (GE Healthcare, Waukesha, WI, USA) for 30 min at room temperature (in the dark). Proteolytic digestion (Supporting Information Fig. S1) was initiated by adding 2 μL of modified porcine trypsin (0.02 μg/μL) (Promega, Madison, WI, USA). The sample was subsequently incubated overnight at 37°C, after which the tryptic digestion was terminated by adding TFA (Fluka, Buchs, Germany) to a final concentration of 0.5% (v/v). After centrifugation at 15 000 × *g* for 10 min the supernatant was cleaned by binding to a SupelClean™ LC-18 1-mL SPE column (Supelco, Bellefonte, PA, USA) equilibrated with 0.1% TFA. The peptides were eluted from this column with 84% ACN (HPLC Supra-gradient, Biosolve, Valkenswaard, The Netherlands) containing 0.1% formic acid (FA) (Merck, Darmstadt, Germany), dried during vacuum centrifugation, and dissolved in 40 μl 0.1% FA prior to LC-MS analysis.

2.5 Comparative LC-MS^E and data dependent LC-MS/MS

For peptide separation, a nanoAcquity UPLC system (Waters, Manchester, UK) was used with a BEH C18 column (75 μm × 25 cm with 1.7 μm particles, Waters, UK) and a 65 min linear gradient from 3 to 40% ACN (in 0.1% FA) at 200 nL/min and the eluting peptides were injected on line into a Synapt Q-TOF HDMS instrument (Waters). MS analyses were performed in positive mode using electrospray ionization (ESI) with a NanoLockSpray source. As lock mass, [Glu^1] fibrinopeptide B (1 pmol/μL) (Sigma) was delivered from a syringe pump (Harvard Apparatus, Holliston, MA, USA) to the reference sprayer of the NanoLockSpray source at a flow rate of 0.2 μL/min and the lock mass channel was sampled every 30 s. Accurate mass

LC-MS data were collected with the instrument operating in either the MS/MS or MS^E mode for data-dependent acquisition (DDA) or data-independent acquisition (DIA). MS^E (DIA) analyses were used for all quantification (24 runs), while DDA MS/MS was used on a few samples to separately confirm peptide identifications. For MS^E, data were acquired collecting spectra every 0.6 s with alternating low (6 eV) and elevated (ramp from 15 to 35 eV) energy over a 140–1900 m/z range. DDA was performed by peptide fragmentation on the three most intense multiply charged ions that were detected in the MS survey scan (0.6 s) over a 300–1400 m/z range with an automatically adjusted collision energy based on the observed precursor m/z and charge state, and using a dynamic exclusion window of 60 s.

2.6 Database construction and data analysis

LC-MS/MS and MS^E data were processed using Proteinlynx Global Server software (PLGS version 2.4, Waters) and per LC-MS run the resulting list of masses containing all the fragment information was searched against the TAIR9 protein sequence database (TAIR9_pep_20090619 downloaded from The Arabidopsis Information Resource (TAIR, www.arabidopsis.org) as part of the TAIR9 Arabidopsis genome release). The annotation of r-protein genes in TAIR9 was updated manually based on published data [23, 24, 28, 40, 41] (Arabidopsis Information Resource (TAIR), http://www.arabidopsis.org; Arabidopsis Transcriptome Genomic Express Database, http://signal.salk.edu/cgi-bin/atta) and recent sequence based data (Hummel et al., manuscript in preparation). For MS^E, the search was performed using the following parameters: a minimum of five fragment ions per peptide and a minimum of nine fragment ions per protein, a minimum of one peptide match per protein and a maximum of one missed trypsin cleavage. Furthermore, we used (i) Carbamidomethylation (Cys) as fixed modification; (ii) Deamidation (NQ), Oxidation (M), and acetylation (N-terminus of the protein) as variable modifications; and (iii) a protein false discovery threshold of 4%. The protein false discovery rate was determined automatically in PLGS by searching the randomized TAIR9 database. For DDA analysis, the peptide tolerance was set to 30 ppm and a fragment tolerance of 0.05 Da. Carbamidomethylation (Cys) was used as a fixed modification and Deamidation (NQ), Dioxidation (M), and Oxidation (M) as variable modifications. The AutoMod option was applied as secondary search to the database search results with a maximum of one missed trypsin cleavage and a nonspecific secondary digest reagent were chosen. Finally, the DDA and MS^E outputs of the separate runs were merged in Excel. Protein identification was considered accurate when a protein (paralog) was assigned based on at least two proteotypic peptides. In the DDA analyses, single peptides were only kept if the ladder score was above 50. For MS^E analyses, proteins that were certified with one peptide were accepted at a peptide-score above 6 in addition to filtering at a false discovery rate of 4%, yielding a maximum false discovery rate of 2% after filtering.

2.7 Protein quantification using Progenesis

For quantitative analyses, the MS^E data were processed in Progenesis LC-MS V2.6 (Nonlinear Dynamics, Newcastle, UK), which transformed the raw high-resolution profile data with lock-spray mass-calibration into a custom mzNLD format and extracted peptide intensity features from MS^E data. The LC-MS^E chromatograms of all 24 (all 12 samples were injected twice, Supporting Information Fig. S1) acquired datasets were aligned against a chosen reference run (run O6 MSe1, arbitrarily chosen as the best representative, due to highest resolution and therefore presumed to have the lowest number of missing data points). Retention time alignment by warping allowed the creation of a single aggregate peak map containing all peak data from all samples. After peak detection on the aggregate map, the peak intensities were determined for each detected individual peak per run. The peak intensity data were further normalized using an approach modified from the internal Progenesis approach (see below). Peptide identification results from Proteinlynx database searches of MS^E data were imported into Progenesis for linking identified peptides to their corresponding peak features. The generated feature table, with peak intensities and (as far as identified and matched) peptide annotations, was exported and further processed in Excel. For intensity normalization, we first removed the features that matched to the FLAG peptide, keratin, and trypsin. From the remainder, we combined features that mapped to the same peptide sequence (e.g. 2+ and 3+ charged, intensities were summed). Subsequently, an offset of 1 was added to the raw intensities (to limit the variation in the low intensity data range) and thereafter the median absolute deviation (MAD) robustness selection and normalization approach from Progenesis (http://www.nonlinear.com/support/progenesis/lc-ms/faq/how-normalisation-works.aspx) was reproduced in Excel, see Supporting Information Table S3. In short, a normalization factor was calculated based on the average of peak intensity ratios for each run versus the reference, after removing the outliers (i.e. the majority of differential peaks). Before further statistical analyses, the intensity values were transformed to a base-2 logarithmic value. Supporting Information Fig. S2 reports the workflow used during the different phases of the analysis.

2.8 Statistical analysis and bioinformatics LC-MS^E and LC-MS/MS analysis

Normalized data were analyzed for univariate statistics using the R language environment for statistical computing (http://www.r-project.org) version 2.11.1 and Bioconductor release 2.6 (http://www.bioconductor.org). Significance of

differential expression per peak was analyzed using the LIMMA package [42]. The obtained *p*-values were corrected for multiple testing using the Benjamini-Hochberg (BH) procedure [43], yielding *q*-values. Lists of *q*-values were transferred to Microsoft Excel™ and sorted/filtered.

Multivariate analysis was performed with SIMCA P+ software (Umetrics, Umeå, Sweden). Logarithmic data were scaled to unit variance before PCA and projection on least squares-differential analysis (PLS-DA). This analysis reports a Variable Importance Parameter (VIP) with a 95% confidence level. The VIP score minus 1.8 × standard error (SE) was used as multivariate significance value between SRibS (6% sucrose treated) and RibO (No supplements treated) samples. The RibO1 sample was removed from the dataset in the final PLS-DA analyses, because of unexplained outlier behavior.

2.9 RNA analysis

RNA was purified from crude extracts by guanidine-HCl precipitation followed by cleanup using RNeasy columns (Qiagen, Venlo, The Netherlands) as described by Kawaguchi et al. [44]. The RNA purity and integrity were confirmed by using Nanodrop1000 spectrometry (Nano-Drop Technologies, Wilmington, DE, USA) and gel electrophoresis. For real-time quantitative PCR analysis, genomic DNA was removed using pretreatment of the total RNA with DNase I (Fermentas) and cDNA was synthesized using anchored oligo-T primers (Biolegio, Nijmegen, The Netherlands) and random hexamers (Fermentas). Complementary DNA was synthesized using M-MuLV reverse transcriptase (Fermentas) according to the manufacturer's instructions. Real-time PCR was performed using ABIPrism7900HT Sequence Detector using Power Cybergreen chemistry (Applied Biosystems, Rotkreuz, Switzerland). Expression levels were calculated relative to *PROTEIN PHOSPHATASE 2A SUBUNIT A3* (*PP2AA3*, AT1G13320) levels using the Q-gene method that takes the relative efficiencies of the different primer pairs into account [45]. Primers were designed according the recommendations of the PCR master-mix manufacturer (Applied Biosystems). For microarray analysis, the RNA was analyzed as above and qualitatively assessed and quantified using an Agilent 2100 Bioanalyzer with the RNA 6000 Nano Labchip kit (Agilent, Santa Clara, CA, USA). RNA was processed and cRNA synthesized according to the 3′ IVT Express kit and hybridized on the ATH1 GeneChip (Affymetrix, High Wycombe, UK). Data from the mRNA profiling experiment were analyzed statistically using the R language environment for statistical computing (http://www.r-project.org) version 2.11.1 and Bioconductor release 2.6 (http://www.bioconductor.org). Differentially expressed genes were identified using the LIMMA package [42]. A posterior residual standard deviation was employed [42] independently for each treatment and the contrast between control- and sucrose-treated samples was determined (change in response to 6% sucrose compared to the change in response to no sucrose). The obtained *p*-values were corrected for multiple testing errors using the BH procedure [43], yielding *q*-values. Lists of *q*-values were transferred to Microsoft Excel™ and sorted. The probe set sequences were aligned to the TAIR9 gene model database of transcripts (Supporting Information Table 5).

3 Results

3.1 Ribosome isolation

The aim of this study was to investigate whether quantitative changes could be detected in the r-protein composition of the ribosome population, in relation to low (no supplements) or high (6%) sucrose growth conditions. Rosette leaves of 4- to 5- wk-old transgenic *A. thaliana* 35S:HF-RPL18B [33] plants were harvested from three independent batches of plants (Supporting Information Fig. S1) and incubated for 24 h in liquid half times Murashige-Skoog media with or without the addition of 6% sucrose (w/v). High sucrose levels were shown to repress translation of the *bZIP11* and other S1 group transcription factor mRNAs [35]. Previous research has shown that translation of the *bZIP11* transcription factor mRNA is regulated by sucrose. In the presence of high sucrose levels, a ribosome stalling complex is formed in a process that requires synthesis of the conserved uORF2 encoded sucrose control (SC) peptide [35]. Likely, ribosome intrinsic or associated proteins are responsible for this evolutionarily conserved sucrose dependent stalling in a process that requires the SC peptide. Possibly, the ribosome r-protein composition changes in response to sucrose in a way that affects *bZIP11* mRNA translation. Affinity isolation of ribosomes was performed with the immunotagged RPL18B *A. thaliana* line, as described in Zanetti et al. [33]. Initial MS analysis of trypsin digested ribosomes isolated from untreated rosette leaves confirmed that the extracts contain mainly r-proteins. No major cytosolic contamination was detected in the ribosomal preparations as determined by Western blotting using the cFBPase antibody. Very limited levels of proteins were immunoprecipitated from wild-type plants (Col-0) lacking the RPL18B transgene, except for low levels of very high molecular weight proteins of unknown nature, as shown by silver stained SDS-PAGE (Supporting Information Fig. S3). Substantial levels of rRNA and mRNA were present in the ribosomal extracts as determined by q-PCR, confirming that the immunopurified ribosomal complexes includes ribosomes engaged in translation. Sucrose treatment efficiently triggered the altered expression of several previously studied marker genes (Supporting Information Fig. S4).

3.2 Peptide identification

For LC-MS analysis immunopurified, r-proteins were precipitated with acetone, digested with trypsin, and peptides purified using C18 SPE for LC-MS analysis. Peptide

identification was based on DIA (MS^E) as well as DDA (MS/MS) analysis; the 12 extracts (six control-treated (CON) and six sucrose (6%) treated (SUC)) were analyzed in duplicate in LC-MS^E mode (Supporting Information Fig. S1) with alternating low and high collision energy, as described in Refs. [46–48]. In addition to MS^E mode, some extracts were also analyzed in MS/MS mode to confirm peptide sequences identified by MS^E and to complement MS^E identifications with MS/MS information. Supporting Information Fig. S2 reports the workflow used during the different phases of the analysis. The peptide fragmentation information, as acquired by the mass spectrometer in MS^E as well as MS/MS mode, was matched to the TAIR9 Arabidopsis genome database using the PLGS software package. In total, 52 102 search hits were accumulated from the MS^E runs and additional MS/MS runs (Supporting Information Table S1). In this total number large redundancy is present due to the repeated detection of peptides in several samples, the matching of single peptide sequences to multiple (paralogous) proteins and also the presence of derived peptides as a result of in-source fragmentation during ESI-MS. Filtering of this redundancy was done at several levels: removing redundancy at the peptide level resulted in a total number of 4127 sequences. From this, 2323 were original sequences and 1804 were sequences derived from in-source decay. Filtering at a high stringency peptide score equal or higher than six, resulted in 2294 total sequences of which 1051 from original and 1243 from in-source decay. At the protein level, these peptides were matched to 511 predicted proteins located at 392 gene loci. Of the 392 different gene loci, 204 are known components of the ribosome, see Supporting Information Table S2A and S2B. With on average nine original peptide sequences (17 total including derived sequences) matched per protein, this provides an average sequence coverage of 22.7%. The high number of peptides matched per protein is a typical characteristic of the MS^E mode of acquisition. In contrast to classical MS/MS where multiple charged peaks are selected for fragmentation, MS^E mode performs a parallel fragmentation of all eluting peptides at the same time. As no precursor selection is performed, more peptides can be identified. Furthermore, in-source decay and neutral loss fragments of ionized peptides are also detected and matched to a protein sequence. The detection of in-source decay fragments provides additional confidence for the identification of a particular peptide sequence [47, 48].

The list of identified proteins can be separated in a set of known ribosomal constituents (204 gene loci) and other proteins (188 loci). A summary on identification numbers is presented in Table 1. For 166 of 204 identified known ribosomal constituents at least two or more proteotypic peptide sequences were matched (including paralogs with identical proteins sequence). These 166 known ribosomal constituents represent 163 r-proteins and three RACK1 paralogs. The 163 r-proteins represent 69% of all 237 *A. thaliana* encoded r-proteins. The protein coverage for the set of known r-proteins was higher than the total average being 32% with on average ten original peptide sequences matched per protein (26 peptides including derived sequences as well). In Supporting Information Table S1, also, a histogram and scatterplot presenting the frequency distribution of the false discovery rate (FDR) and the relation to peptide and protein scores is presented. All r-proteins have been detected with a protein FDR below 0.01%. Proteins with a higher FDR were either ribosome associated or background identified proteins.

One hundred and eighty-eight non-r-proteins were identified in our datasets (Table 1). The protein coverage for the set of non-r-proteins was lower than the total average being 11% with on average seven original peptide sequences matched per protein (eight peptides, including derived sequences). The majority of these proteins are nuclear encoded (185 of 188 proteins). Some proteins, like RuBisCo small subunit proteins are highly expressed and can therefore be suspected to be translated by the immunoprecipitated ribosomes. However, at this stage, a functional role of the non-r-proteins in ribosomal biogenesis, nuclear export, or translation or the regulation thereof remains to be established.

3.3 Label-free quantitative analysis of the MS^E data by peak alignment

For quantitative analysis, the LC-MS^E raw data were used, as this acquisition mode provides a maximum coverage of the chromatographic peak shape of all eluting peptide ions,

Table 1. Protein identifications data of ribosomal an nonribosomal proteins identified by MS^E and DDA

	r-proteins and RACK1	r-proteins and RACK1[a)]	Nonribosomal proteins
Number of genes (Loci) identified	204	166	188
Number of gene models identified	275	214	236
Average protein sequence coverage (%) of identified proteins	31	32	11
Average number of peptides per identified protein	24	26	8
Average number of in-source decay fragments per identified protein	14	15	2
Average number of original peptides per identified protein	10	11	7
Average total DDA score of identified proteins	270	281	89
Average total IA score[b)] of identified proteins	168	175	46

a) At least two matched proteotypic peptide sequences.
b) IA score = scores of peptide matches obtained in MS^E database search.

in contrast to MS/MS mode. The LC-MS^E raw data were analyzed using Progenesis LC-MS software. This analysis pipeline enables label-free quantitation of all detected peaks, independent of being identified or not. Supporting Information Fig. S2 reports the workflow used during the different phases of the analysis. Progenesis performs interactive peak matching and warping of LC-MS peak maps before the actual peak detection and quantitation. Peak patterns were aligned starting with circa 10 manual landmarks per LC-MS run followed by automatic vector detection. Subsequently, LC-MS patterns were stretched in retention time domain (warped) according to these match vectors and an aggregate peak map was constructed based on all aligned LC-MS patterns. Then, peak detection was performed on the aggregate image and peak intensity data were collected from each aligned run for all detectable peaks. In total, 5334 peaks were detected with Progenesis. For the majority of these peaks intensity, data were available from all 24 LC-MS runs. The identification from both MS^E and MS/MS acquisition have been used to annotate the quantification features as far as they were identified by either of both methods. In order to link peak intensity information to protein identifications, the database search results of MS^E data from PLGS were imported into Progenesis. In addition, MS/MS data from DDA runs were loaded and aligned in Progenesis. For these runs, the MS/MS peak lists were generated in Progenesis and database search was performed with MASCOT and reimported into Progenesis. In summary, from a total of 5334 features, 1122 were identified by MS^E and/or MS/MS. As some peptide sequences matched with more than one peak (in cases of multiple charge states), these peaks were combined and the intensity data were summed. This resulted in 752 peptide sequences that were matched to one or more peaks in the quantitation table. For 4212 detected and quantified peaks, no identification was matched. In order to correct for differences in ribosome extraction efficiency and LC-MS sample loading, a normalization procedure was applied to both the identified as well as unidentified peaks. Prior to normalization, peaks that were identified as keratin or 3X FLAG® Peptide (Sigma) were removed. After summing of identical peak identification intensities, an offset = 1 was added to limit the variation in the low intensity data range and peak intensities were normalized according to the MAD normalization method adapted from Progenesis (Supporting Information Table S1). Figure 1 shows boxplot distributions of the peak intensities per sample prior to and after normalization. The normalization results in a more homogeneous distribution of peak intensities, where the median of distributions is similar in all samples, and the spread in low intensity peaks has been substantially reduced.

3.4 Differential r-protein composition of the ribosome in response to sucrose feeding

To globally depict the intensity variance between the sucrose-treated and control ribosomal preparations, PCA was performed using all matched peaks (identified as well as non-identified). In the PCA plot, as displayed in Fig. 2A, 44% of total variance was explained by the first two principal components. The sucrose-treated (RibS) and control samples (RibO) are clearly separated, mainly on the first component (explaining 26% variance). Furthermore, the replicate runs of each sample and the replicate extracts from each treatment appear to cluster together, indicating that the variance within the replicate extractions and replicate runs is much smaller than the variance between treatments and biological replicates. The PCA plot indicates that the sucrose and nonsucrose-treated samples are different. In order to optimally differentiate between sucrose and nonsucrose samples a multivariate PLS-DA analysis was performed to maximally

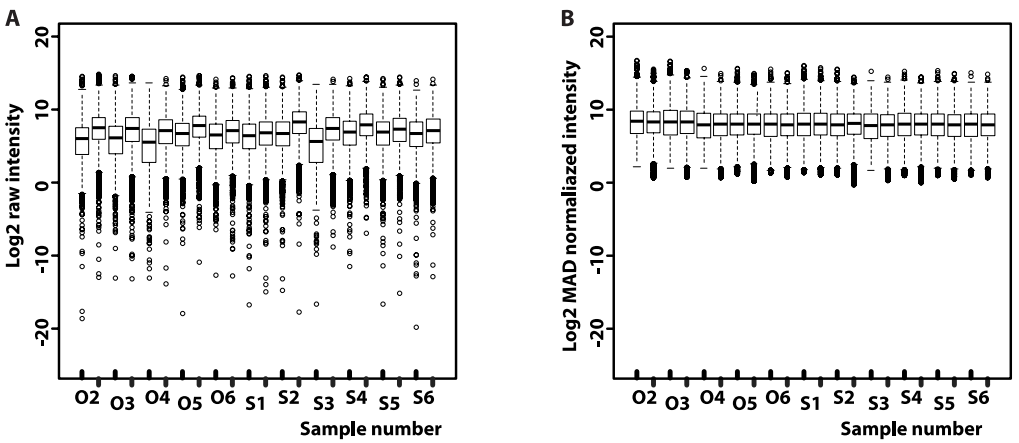

Figure 1. MAD normalization gives highly comparable data sets. (A) Feature intensities prior to normalization and (B) normalized feature intensities after MAD normalization (offset = 1). Samples treated with O = no supplements (0% sucrose) or S = 6% sucrose. The two technical replicates are represented by black and gray ticks at the *x*-axis, respectively. Boxes represent the interquartile range and the thick line represents the median of the values. The dashed lines represent values within 1.5 times the box width and circles represent outliers outside this range.

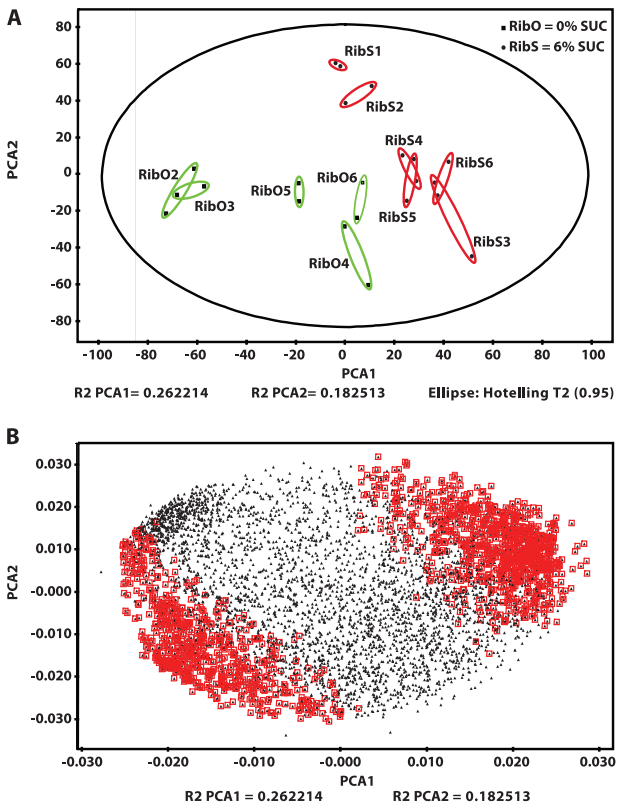

Figure 2. Sugar treatment affects the riboproteome as displayed by PCA analysis. Data generated by the analysis of the immunopurified ribosomal preparations from sugar treated and control leaves. (A) PCA scores (PCA1 and PCA2). Ellipses encircle technical replicates, green, control; red, sugar treated. (B) Loadings plot. The data points with a positive value for Variable Importance Parameter (VIP) score minus 1.89 × standard error (VIP-SE score) are color marked. R2 PCA1 and R2 PCA2 indicate the percentage of variance that can be explained in the first two dimensions.

separate both classes [49]. Twenty-two of 24 replicates were included in this analysis. One of the samples (RibO1) was removed from the dataset in the final PLS-DA analysis, because of unexplained outlier behavior. This analysis reports a VIP (95% confidence level) indicating per data point the strength of separating the two classes. The data points with a positive value for (VIP score minus 1.89 × SE) are considered as significant contributions (SIMCA P+, Umetrics) and these are color marked in the loading plot of the PCA in Fig. 2B. Peaks with VIP-SE scores above 0 are well separated on the first PCA component. The analysis shows a significant change in ribosome composition in response to sucrose. However, the majority of the quantified features are not significantly responsive to sucrose feeding (i.e VIP-SE score <0, Supporting Information Table S4A). In addition to multivariate statistics, a linear model-based analysis of the normalized data was performed, with the goal of detecting peptides undergoing significant changes in abundance between sugar- and control-treated leaves. This analysis was performed following the PLS-DA. The resulting BH corrected *p*-values (*q*-values) from the LIMMA analysis were transferred to Excel (Supporting Information Fig. S2). The significant correlation between the VIP-SE score and the log of the *q*-value is displayed in Supporting Information Fig. S5.

Focussing on the 1122 features (out of 5334 total) that were identified, we merged the quantitative data to 752 peptide sequences. From these peptides only a subset was unique per r-protein paralog (see http://www.arabidopsis.org/browse/genefamily/athr.jsp). We classified proteins as differentially present only if they were identified by two unique peptides (confirmed by PatMatch, http://arabidopsis.org/cgi-bin/patmatch/nph-patmatch.pl, TAIR9), intensity changing more than 41% (0.5 on a $\log_2$ scale) and indicated significant both by multi- and univariate statistics (VIP-SE score >0, *q*-value <0.05). These criteria are reasonably strict and possibly some differential r-proteins were overlooked. Of the 204 r-constituents identified in this study, of which 166 with paralogous-specific peptide sequences, 13 r-constituents paralogs changed significantly in response to sucrose (Table 2 and Supporting Information Table S4B). These results show that the ribosome composition changes in response to sucrose treatment. Interestingly, for several of the changing r-protein, paralogs mutants have been reported that show distinct growth phenotypes [50, 51]. Also the protein abundance of RACK1A [52, 53], a scaffold protein on the 60S ribosomal subunit, increases upon sucrose treatment. Figure 3 shows the resulting changes in r-protein families RPS3a, RPS7, RPL8, and the RACK1 family, respectively. The fold changes of multiple proteotypic peptides per paralog are more or less similar. However, there are some outliers, for example RPS7C peptide DKNAEPT. This long peptide actually had the lowest absolute peak intensity from the (proteotypic) selected set, resulting in a less accurate a peak quantitation compared to the other peptides. As can be seen in Fig. 3, only the levels of RPS3aA, RPS7C, RPL8C, and RACK1A and not their paralogs are changing in response to sucrose treatment, using our stringent criteria. These data indicate that the incorporation abundance of specific r-protein paralogs into newly synthesized ribosomes is differentially regulated in response to sucrose.

3.5 Differential presence of r-proteins in the ribosome cannot be explained by transcriptional regulation of r-protein genes

To understand the mechanism of r-protein regulation within the ribosome, microarray of the steady-state mRNA population was performed. Interestingly, most r-protein genes are upregulated by sucrose treatments on the transcriptional level, except RPL19C, but also for other r-protein paralogs and RACK1 paralogs an upregulation on steady-state mRNA levels is observed (Table 2 and Supporting Information Table S5). These results confirm previous publications

Table 2. Sucrose mediated changes in r-protein and RACK1A abundance

Protein	Gene model	Log_2 fold change steady-state mRNA	*q*-value steady-state mRNA[a)]	Peptide sequence	Log_2 fold change peptide	*q*-value peptide[a)]	VIP-SE score
RPS8A	AT5G20290.1	0.47	3.55×10^{-2}	LDTGNYSWGSEATTR	0.78	1.29×10^{-2}	0.69
				VLDVVYNASNNELVR	0.69	4.45×10^{-4}	1.11
RPS3aA	AT3G04840.1	1.06	1.27×10^{-3}	VFEVSLADLQNDEDNAYR	1.14	8.80×10^{-7}	1.81
				VDRPADETMVEEPTEIIGA	0.65	7.73×10^{-3}	0.72
RPL12C	AT5G60670.1	1.57	4.44×10^{-4}	ELSGTVKEILGTCVSVGCTVDGKDPK	1.29	4.17×10^{-5}	1.51
				DPKDLQEEINSGDIDIPNE	0.72	4.82×10^{-3}	0.90
				DLQEEINSGDIDIPNE	0.87	2.28×10^{-4}	1.01
RPL19A	AT1G02780.1	0.53	3.60×10^{-2}	VWLDPNESSDISMANSR	0.75	1.28×10^{-3}	1.10
				GPGGDVAPVAAPAPAATPAPTAAVPK	0.62	1.39×10^{-3}	1.08
RPL19B	AT3G16780.1	1.68	9.07×10^{-5}	LAQGPGGGETTTPAGAPQQPEVTK	0.71	4.76×10^{-4}	1.01
				LAQGPGGGETTTPAGAPQQPEVTKK	1.08	1.04×10^{-2}	0.62
RPL19C	AT4G02230.1	0.21	5.34×10^{-1}	GPGGDIPAAAPPAQTAEVPAK	0.97	1.56×10^{-2}	0.51
				GPGGDIPAAAPPAQTAEVPAKK	1.03	1.09×10^{-3}	1.00
RPL30B	AT1G77940.1	1.21	2.30×10^{-4}	LILISTNCPPLR	0.93	3.28×10^{-5}	1.56
				LILISTNCPPLRR	1.09	1.56×10^{-2}	0.55
RPL8C	AT4G36130.1	0.63[b)]	3.71×10^{-3} [b)]	SIPEGAVICNVEHHVGDR	0.72	4.93×10^{-2}	0.17
				ASGDYAIVIAHNPDNDTSR	0.90	1.72×10^{-4}	1.26
RACK1A	AT1G18080.1	0.67	1.39×10^{-2}	LWDLAAGVSTR	0.78	6.38×10^{-4}	1.21
				FSPNTLQPTIVSASWDK	0.87	8.60×10^{-4}	1.00
				STLAGHTGYVSTVAVSPDGSLCASGGK	0.88	2.65×10^{-4}	1.31
RPL28A	AT2G19730.1/2	1.17	5.61×10^{-4}	TVTIQAADKDQAVVLATTK	0.65	3.50×10^{-3}	1.30
				AVANQVVDNYYRPDLKK	0.76	3.09×10^{-4}	1.09
RPS12A	AT1G15930.1/2	0.78	1.39×10^{-3}	VAQLVVLAEDCNQPDYVK	1.18	9.03×10^{-5}	1.38
				DFGEETTALSIVNK	0.74	4.82×10^{-3}	0.76
RPS12C	AT2G32060.1/2/3	1.80	1.55×10^{-4}	NAQLCVLAEDCNQPDYVK	1.18	6.21×10^{-6}	1.60
				DFGEETTALNIVK	0.75	2.52×10^{-4}	1.24
				DFGEETTALNIVKK	0.58	4.92×10^{-4}	1.29
RPL22B	AT3G05560.1,2/3	0.96	7.41×10^{-4}	AGALGDSVTITR	0.56	2.64×10^{-3}	1.04
				YFNIAENEGEEED	0.85	2.48×10^{-4}	1.05
RPS7C	AT5G16130.1	1.73	2.75×10^{-4}	DKNAEPTECEEQVAQALFDLENTNQELK	1.43	2.46×10^{-3}	0.77
				TLTSVHEAMLEDVAFPAEIVGK	0.61	6.06×10^{-2}	0.13
				DVVFEYPVEA	0.68	7.76×10^{-4}	1.16

The changed steady-state mRNA levels in response to sucrose treatment determined by microarray analysis are indicated as log_2 fold change steady-state mRNA (log_2 intensity 6% sucrose treated – log_2 intensity no supplements treated). The changed peptide abundance levels in response to sucrose treatment determined by LC-MS^E are indicated as log_2 fold change peptide (log_2 intensity 6% sucrose treated – log_2 intensity no supplements treated).

a) *q*-values are associated with the relative change in signal in the microarray experiment or LC-MS^E analysis. Details about the differential r-protein and RACK1 families are presented in Supporting Information Table 4b. The steady-state mRNA levels shown in this table is a subset of the microarray data of which the complete set is presented in Supporting Information Table 5.

b) Probe on ATH1 array not specific enough to discriminate between different paralogous RPL8 genes.

in which r-protein regulation in response to sugar availability was reported [6, 54]. The microarray data confirms the real-time PCR analysis shown in Supporting Information Fig. S4. For the r-proteins RPL12C, RPL30B, and RPS7C, their increased protein abundance in the immunoprecipitated ribosomes can be explained by higher steady-state mRNA levels. Their paralogous genes are not upregulated at the steady-state mRNA level to corresponding levels (Table 2 and Supporting Information Table S5). For the other differential r-proteins and RACK1A, a similar phenomenon is not observed. This is especially true for RACK1A, RPS8A, and RPL22B for which an increased protein abundance is observed by LC-MS^E while the steady-state mRNA levels of their paralogs increase more in response to sucrose feeding. For RPS3a and RPL28 family members, the regulation is identical for the paralogous genes at the steady-state mRNA level while an increased protein abundance of RPL3aA and RPL28A in the immunopurified ribosomal isolates is observed. The differential presence of r-proteins in the ribosome can thus not simply be explained by differential mRNA steady-state levels of the corresponding r-protein or RACK1 genes (Table 2 and Supporting Information Table S5).

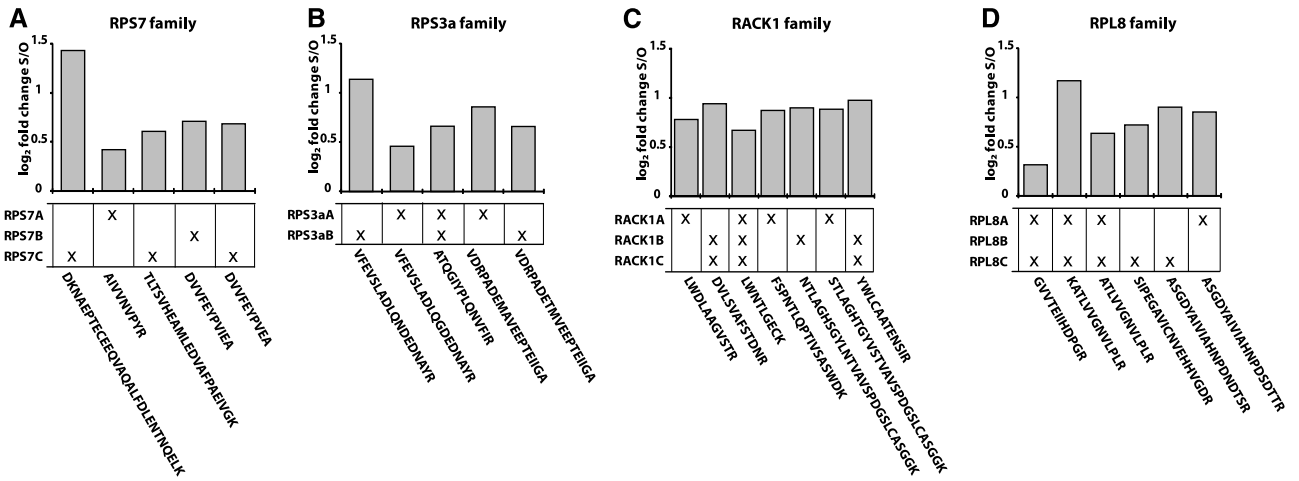

Figure 3. Ribosomal protein levels change in response to sucrose treatments. Changed levels of individual peptides in response to sucrose feeding are indicated. Only peptides with a significantly changed level (q-value <0.05 and a VIP-SE score >0) are depicted. The matches to the individual paralogous r-proteins are indicated in the matrix below the graphs. We classified proteins as differentially present only if they were identified by two or more peptides significant according to both above mentioned criteria and with an average change $\log_2$ (fold change) exceeding 0.5 (41%). (A) RPS7 r-protein family, (B) RPS3a r-protein family, (C) RACK1 family, and (D) RPL8 r-protein family.

4 Discussion

The ribosome is a large multiprotein-RNA complex consisting of 79 different r-proteins and four rRNAs. In *A. thaliana*, each r-protein is encoded by two to six different r-protein genes [23] and inspection of the literature and expression databases show that these genes generally are expressed [30]. The available 80S ribosome structures ([10–12] and references therein) show that only one r-protein paralog is present in each ribosome. Given the number of *A. thaliana* r-protein paralogs and assuming independent ribosome incorporation, theoretically more than 10^{34} different ribosome types can be assembled in an *A. thaliana*. Such stunning potential heterogeneity raises several questions, foremost whether all the different paralogs are incorporated into ribosomes since several reports indicate that r-proteins might have functions outside the ribosome [55–59]. In view of this heterogeneity, it is important to establish whether the ribosome protein composition changes in response to endogenous or environmental signals. These questions can only be answered by studying the ribosome composition in living cells, as presented in this manuscript. Transgenic plants harboring His-Flag-tagged RPL18B were used to purify actively translating ribosomes from living cells by rapid immunopurification [33]. According to Ref. [33], this immunopurification method yields 40S and 60S ribosomal subunits as well as 80S monosomes and small and large polysomes with similar sedimentation characteristics as polysomes isolated by ultracentrifuge-concentrated fractionation. Polysomal mRNA extracted from immunopurified ribosomes can be used for large-scale mRNA profiling [33, 34], confirming that these extracts contain actively translating ribosomes. Our proteomic characterization using LC-MS^E shows that the vast majority of the 237 encoded *A. thaliana* r-proteins are present in the ribosome pool. Some r-proteins are absent from the list of identified proteins and their absence can be explained by the extreme small size of these proteins (e.g. RPL41 family members are only 25 aa long) or by the high lysine and arginine content (e.g. RPL39 family members have approximately 40% basic amino acids). LC-MS^E detection of peptides of such proteins by trypsin digestion is challenging. With these exceptions, nearly all r-proteins encoded by the *A. thaliana* genome have been detected in the ribosome preparations. This shows that nearly all r-protein paralogs are present in translating ribosomes.

The list of identified proteins also includes non-r-proteins (see Supporting Information Table S2A and S2B). These non-r-proteins may have functions in translation, such as elongation factor 1 alpha/beta (AT1G07920/AT2G18110), Hsp70 (AT3G12580), or isoleucyl-tRNA synthetase (AT4G10320). Other non-r-protein may be retrieved due to their involvement in ribosomal biogenesis, maturation, or because they are actively translated by the purified ribosomes. Non-r-proteins may also be present due to nonspecific binding during the affinity purification procedure, for example RuBisCO small subunit (AT5G38410/AT5G38420/AT5G38430) or LIGHT HARVESTING COMPLEX proteins (AT1G15820, AT1G29910, AT1G29920, AT1G29930). For many non-r-proteins, it is difficult to discriminate between specific or nonspecific binding but clearly RuBisCO large subunit protein is nonspecific as this protein is encoded by the plastid genome and translated by plastid ribosomes. RuBisCO is the most abundant protein in plants and is infamous as a "sticky protein" in many affinity enrichment procedures. That the isolated protein extract is dominated by r-proteins can be concluded from the large difference in distribution of

the number of identified peptides per protein (average is 24 for r-proteins compared to 8 for non-r-proteins, the average coverage is 31.2% for r-proteins compared to 11.3% for non-r-proteins and the average sum of MS^E score is 168 for r-proteins compared to 46 for non-r-proteins, see Table 1 and for detailed histograms of these distribution see Supporting Information Table S2B). These distributions indicate that non-r-protein ribosome associated proteins are present at lower levels than the r-proteins.

This study documents changes in *A. thaliana* cytosolic r-protein composition in response to sucrose feeding. Sucrose feeding has tremendous impact on physiology and gene regulation and similar sucrose treatments were shown to specifically affect the translation of bZIP11 and other S1 group proteins [35, 60, 61]. Specific r-protein paralogs change in abundance, such as RPL28A and RPS7C, which implies that different r-protein paralogs are incorporated into the ribosome depending on growth conditions. The detected changes in paralog protein abundance are limited. Fold changes usually do not exceed a 2.7-fold. This indicates that multiple r-protein paralogs are incorporated in ribosomes in both conditions, whereas the relative ratios in ribosomes change upon sucrose feeding. Alternatively, incorporation differences could be much larger in restricted responsive tissues or cells of the leaves. These results indicate that *A. thaliana* adapts its r-protein composition in response to a changing environment. R-protein composition changes have been reported for individual proteins in different organisms [62, 63]. Here, simultaneous changes of the levels of several r-proteins are reported. This indicates an underlying regulatory mechanism responsible for a rearranged ribosomal proteome in response to sugar feeding and possibly to other types of environmental changes as well. For some of the r-protein paralogs and RACK1 that change in response to the sucrose feeding, mutants are identified that are affected in plant development and physiology [50–53, 64]. A majority of the reported mutations in *A. thaliana* r-protein genes cause relatively moderate and defined phenotypic deviations, which indicates defined roles for individual r-protein paralogs. In the asymmetric leaves 1 (*as1*) mutant background, suppressor mutations in several r-protein genes were obtained that cause altered leaf patterning. The transcription factor AS1 promotes adaxial identity of leaves by positive regulation of transcription factors that specify adaxial fate during leaf development [65] and mutations in *as1* disrupt development of cotyledons, leaves, and flowers [66]. Mutations in r-protein paralogs, such as *PIGGYBACK (pgy1 RPL10aB*, *pgy2, RPL9B*, and *pgy3, RPL5A*), *asymmetric leaves1/2 enhancer5 (as5, RPL28A)*, and *asymmetric leaves1/2 enhancer6* (*ae6, RPL5A*), enhance the aberrant phenotype of the *as1* mutation and show an altered leaf patterning [51, 67]. Other r-protein gene mutants show narrow pointed or round first and second leaves, known as the POINTED FIRST LEAVES (*pfl*) mutants, *pfl1 (rps18a)* and *pfl2* (*rps13a*) [68, 69]. This indicates differential functionality of the different r-protein paralogs in *A. thaliana*. *RPL4A* mutants show a plethora of developmental defects, such as the *pfl* phenotype and retarded growth [70]. When grown side-by-side, *rpl4a* mutants could not be distinguished from *rpl4d* mutants. In *rpl4a* mutants, *RPL4D* was expressed to higher levels and vice versa, indicating that the loss of one of the *RPL4* genes is compensated by increased expression of the other. This shows that *A. thaliana* adapts by changed expression of r-protein genes in response perceived changes in r-protein levels [70]. Relatively few mutants in *A. thaliana* r-protein genes show embryo-defective phenotypes. Embryo abortion was reported for *RPL8A*, *RPL19A*, *RPL23C*, *RPL40B*, *RPS6B*, *RPS11A*, and *RPL5A* [50, 64]. This indicates that for general translation most r-protein paralogs are redundant but the above-mentioned specific phenotypes of mutations in r-protein genes and our data on changed levels of r-proteins in the ribosome pool clearly indicate that r-protein paralogs can have specific functions.

The findings presented here show that the *A. thaliana* ribosome protein composition changes in response to sucrose treatment. The half-life of mammalian ribosomes is approximately 3 days [71, 72]. In *Chlamydomonas reinhardtii*, the ribosome half-life is approximately 15 h [73] but that of plants is not yet reported. The observed changes in ribosome protein composition are most likely a consequence of the regulation of r-protein synthesis. R-protein mRNA levels are generally coordinately regulated, being upregulated when energy status is high and downregulated when energy is limited (Genevestigator, www.genevestigator.com and reviewed in [74]). Additionally, the translation of r-protein mRNAs is coordinately downregulated by water deficit, oxygen deprivation, and sucrose starvation [44, 54, 75, 76]. However, there are striking exceptions from the observed general patterns. Sucrose treatment results in mRNA upregulation of many r-protein genes, including steady state (Table 2 and Supporting Information Table S5). R-protein synthesis can be regulated by a feedback mechanism as exemplified by upregulation of *RPL4D* in *rpl4a* mutants [70]. The regulatory circuit involves more r-proteins than members of the RPL4 family as indicated by compensatory regulation of *RPS6* in the *rpl4* mutants. However, from the microarray analysis, the differential protein abundance of r-protein paralogs in the ribosomes cannot simply be explained by differential steady-state mRNA levels of the corresponding proteins. This indicates that the r-protein regulation and consequently ribosome biogenesis is more complex than expected and likely occurs at multiple regulation levels including both transcriptional and posttranscriptional regulation mechanisms.

Even within a single day plants experience substantial changes in their growth environment, and depend on effective adjustment mechanisms, for example via the modulation of metabolism. Translation is one of the most energy-consuming processes and it is not surprising that plants adjust translation in response to environmental cues. A dramatic reduction in large polysomes (more than one ribosome per mRNA) can be observed during the dark period of the diurnal cycle [77]. Substantial changes during the diurnal cycle in the translation state of several mRNAs

encoding enzymes of central metabolism were observed by profiling of total mRNA and polysomal mRNA populations, and measurement of corresponding enzyme activities [77,78]. Comparison of total mRNA and polysomal mRNA populations isolated from plant material grown under stressful conditions such as hypoxia, dehydration, and sucrose starvation showed a dramatic effect on polysomal loading and, thus mRNA translation under these conditions [44, 54, 76, 79, 80]. These results show that mRNA translation is highly regulated in response to several different factors including nutrient/energy supply. It remains to be investigated whether the changes in ribosome composition reported here somehow relate to differential mRNA translation. The documented changes in r-protein levels might function in mRNA selection or might affect other aspects of ribosome performance such as kinetics, accuracy, or cellular localization. In recent reports, the ribosome emerges as a signaling platform that has essential functions in cellular signaling pathways, in addition to its function as a protein synthesis supercomplex. For example, the mammalian target of rapamycin (TOR) complexes TORC1 and TORC2 have central roles in linking nutrients and growth factors to metabolism and growth, and it was found that ribosome association of the TORC2 complex is essential for its function [81,82]. Activation of TORC2 protein kinase activity depends on its association with ribosomes, which was stimulated by growth factors via the phosphatidylinositol 3-kinase (PI3K) signaling pathway. The TOR kinase signaling pathway is essential for growth in Arabidopsis as well. We observed that sucrose feeding increases the abundance of RACK1 protein family members on Arabidopsis ribosomes. Interestingly, in animal cells, RACK1 was found to tether the active protein kinase C isoform PKCβII to translating ribosomes [83]. These findings, and others, point to the ribosome as an important regulatory site in cellular signaling events.

This study represents a starting point for investigations on the dynamics of the ribosomal proteome and the underlying regulatory processes. Such studies are relevant for the understanding of translational processes in relation to environmental and developmental changes. The function of individual r-protein paralogs must be studied by genetic analysis of r-protein mutants to clarify their roles in response to stress or energy deprivation. It will be interesting to determine how these processes affect plant performance.

The peptide identification data have been deposited to PRIDE database, http://www.ebi.ac.uk/pride/ (accession numbers 16881–16939).

We are grateful to Professor Julia Bailey-Serres, UC Riverside, Riverside, USA for kindly providing the 35S:HF-RPL18 transgenic line and for her comments on the manuscript. We would like to thank Jolanda Schuurmans for excellent technical assistance. We would like to thank Dr. Bas van Breukelen and Henk van den Toorn, Biomolecular Mass Spectrometry and Proteomics Group, Utrecht University, Utrecht for their comments on the manuscript. This work was supported by grants from the Netherlands Genomics Initiative (NGI), Earth and Life Sciences Foundation subsidized by the Netherlands Organization for Scientific Research (NWO) and Centre for BioSystems Genomics (CBSG).

The authors have declared no conflict of interest.

5 References

[1] Warner, J. R., The economics of ribosome biosynthesis in yeast. *Trends Biochem. Sci.* 1999, *24*, 437–440.

[2] Yamasaki, S., Anderson, P., Reprogramming mRNA translation during stress. *Curr. Opin. Cell Biol.* 2008, *20*, 222–226.

[3] Koch, K. E., Carbohydrate-modulated gene expression in plants. *Annu. Rev. Plant Physiol. Plant Mol. Biol.* 1996, *47*, 509–540.

[4] Ho, S. L., Chao, Y. C., Tong, W. F., Yu, S. M., Sugar coordinately and differentially regulates growth- and stress-related gene expression via a complex signal transduction network and multiple control mechanisms. *Plant Physiol.* 2001, *125*, 877–890.

[5] Rylott, E. L., Gilday, A. D., Graham, I. A., The gluconeogenic enzyme phosphoenolpyruvate carboxykinase in Arabidopsis is essential for seedling establishment. *Plant Physiol.* 2003, *131*, 1834–1842.

[6] Baena-Gonzalez, E., Sheen, J., Convergent energy and stress signaling. *Trends Plant Sci.* 2008, *13*, 474–482.

[7] Ban, N., Nissen, P., Hansen, J., Moore, P. B., Steitz, T. A., The complete atomic structure of the large ribosomal subunit at 2.4 angstrom resolution. *Science* 2000, *289*, 905–920.

[8] Wimberly, B. T., Brodersen, D. E., Clemons, W. M., Morgan-Warren, R. J. et al., Structure of the 30S ribosomal subunit. *Nature* 2000, *407*, 327–339.

[9] Schmeing, T. M., Ramakrishnan, V., What recent ribosome structures have revealed about the mechanism of translation. *Nature* 2009, *461*, 1234–1242.

[10] Armache, J. P., Jarasch, A., Anger, A. M., Villa, E. et al., Localization of eukaryote-specific ribosomal proteins in a 5.5-A cryo-EM map of the 80S eukaryotic ribosome. *Proc. Natl. Acad. Sci. USA* 2010, *107*, 19754–19759.

[11] Armache, J. P., Jarasch, A., Anger, A. M., Villa, E. et al., Cryo-EM structure and rRNA model of a translating eukaryotic 80S ribosome at 5.5-A resolution. *Proc. Natl. Acad. Sci. USA* 2010, *107*, 19748–19753.

[12] Ben-Shem, A., Jenner, L., Yusupova, G., Yusupov, M., Crystal structure of the eukaryotic ribosome. *Science* 2010, *330*, 1203–1209.

[13] Louie, D. F., Resing, K. A., Lewis, T. S., Ahn, N. G., Mass spectrometric analysis of 40 S ribosomal proteins from rat-1 fibroblasts. *J. Biol. Chem.* 1996, *271*, 28189–28198.

[14] Arnold, R. J., Polevoda, B., Reilly, J. P., Sherman, F., The action of N-terminal acetyltransferases on yeast ribosomal proteins. *J. Biol. Chem.* 1999, *274*, 37035–37040.

[15] Lee, S. W., Berger, S. J., Martinovic, S., Pasa-Tolic, L. et al., Direct mass spectrometric analysis of intact proteins of the

yeast large ribosomal subunit using capillary LC/FTICR. *Proc. Natl. Acad. Sci. USA* 2002, *99*, 5942–5947.

[16] Odintsova, T. I., Muller, E. C., Ivanov, A. V., Egorov, T. A. et al., Characterization and analysis of posttranslational modifications of the human large cytoplasmic ribosomal subunit proteins by mass spectrometry and Edman sequencing. *J. Protein Chem.* 2003, *22*, 249–258.

[17] Yu, Y. H., Ji, H., Doudna, J. A., Leary, J. A., Mass spectrometric analysis of the human 40S ribosomal subunit: native and HCVIRES-bound complexes. *Protein Sci.* 2005, *14*, 1438–1446.

[18] Mazumder, B., Sampath, P., Seshadri, V., Maitra, R. K. et al., Regulated release of L13a from the 60S ribosomal subunit as a mechanism of transcript-specific translational control. *Cell* 2003, *115*, 187–198.

[19] Bachand, F., Silver, P. A., PRMT3 is a ribosomal protein methyltransferase that affects the cellular levels of ribosomal subunits. *EMBO J.* 2004, *23*, 2641–2650.

[20] Bailey-Serres, J., Vangala, S., Szick, K., Lee, C. H., Acidic phosphoprotein complex of the 60S ribosomal subunit of maize seedling roots. Components and changes in response to flooding. *Plant Physiol.* 1997, *114*, 1293–1305.

[21] Szick-Miranda, K., Bailey-Serres, J., Regulated heterogeneity in 12-kDa P-protein phosphorylation and composition of ribosomes in maize (*Zea mays* L.). *J. Biol. Chem.* 2001, *276*, 10921–10928.

[22] Chang, I. F., Szick-Miranda, K., Pan, S. Q., Bailey-Serres, J., Proteomic characterization of evolutionarily conserved and variable proteins of arabidopsis cytosolic ribosomes. *Plant Physiol.* 2005, *137*, 848–862.

[23] Barakat, A., Szick-Miranda, K., Chang, I. F., Guyot, R. et al., The organization of cytoplasmic ribosomal protein genes in the arabidopsis genome. *Plant Physiol.* 2001, *127*, 398–415.

[24] Carroll, A. J., Heazlewood, J. L., Ito, J., Millar, A. H., Analysis of the Arabidopsis cytosolic ribosome proteome provides detailed insights into its components and their post-translational modification. *Mol. Cell. Proteomics* 2008, *7*, 347–369.

[25] Giavalisco, P., Wilson, D., Kreitler, T., Lehrach, H. et al., High heterogeneity within the ribosomal proteins of *the Arabidopsis thaliana* 80S ribosome. *Plant Mol. Biol.* 2005, *57*, 577–591.

[26] Williams, A. J., Werner-Fraczek, J., Chang, I. F., Bailey-Serres, J., Regulated phosphorylation of 40S ribosomal protein S6 in root tips of maize. *Plant Physiol.* 2003, *132*, 2086–2097.

[27] Zhang, Z. L., Harrison, P., Gerstein, M., Identification and analysis of over 2000 ribosomal protein pseudogenes in the human genome. *Genome Res.* 2002, *12*, 1466–1482.

[28] Nakao, A., Yoshihama, M., Kenmochi, N., RPG: the ribosomal protein gene database. *Nucleic Acids Res.* 2004, *32*, D168–D170.

[29] Szick, K., Springer, M., Bailey-Serres, J., Evolutionary analyses of the 12-kDa acidic ribosomal P-proteins reveal a distinct protein of higher plant ribosomes. *Proc. Natl. Acad. Sci. USA* 1998, *95*, 2378–2383.

[30] Schmid, M., Davison, T. S., Henz, S. R., Pape, U. J. et al., A gene expression map of *Arabidopsis thaliana* development. *Nat. Genet.* 2005, *37*, 501–506.

[31] Schippers, J. H. M., Mueller-Roeber, B., Ribosomal composition and control of leaf development. *Plant Sci.* 2010, *179*, 307–315.

[32] Komili, S., Farny, N. G., Roth, F. P., Silver, P. A., Functional specificity among ribosomal proteins regulates gene expression. *Cell* 2007, *131*, 557–571.

[33] Zanetti, M. E., Chang, I. F., Gong, F. C., Galbraith, D. W., Bailey-Serres, J., Immunopurification of polyribosomal complexes of arabidopsis for global analysis of gene expression. *Plant Physiol.* 2005, *138*, 624–635.

[34] Mustroph, A., Zanetti, M. E., Jang, C. J., Holtan, H. E. et al., Profiling translatomes of discrete cell populations resolves altered cellular priorities during hypoxia in Arabidopsis. *Proc. Natl. Acad. Sci. USA* 2009, *106*, 18843–18848.

[35] Rahmani, F., Hummel, M., Schuurmans, J., Wiese-Klinkenberg, A. et al., Sucrose control of translation mediated by an upstream open reading frame-encoded peptide. *Plant Physiol.* 2009, *150*, 1356–1367.

[36] Ma, J., Hanssen, M., Lundgren, K., Hernandez, L. et al., The sucrose-regulated Arabidopsis transcription factor bZIP11 reprograms metabolism and regulates trehalose metabolism. *New Phytol.* 2011, *191*, 733–745.

[37] Hanson, J., Hanssen, M., Wiese, A., Hendriks, M. M. W. B., Smeekens, S., The sucrose regulated transcription factor bZIP11 affects amino acid metabolism by regulating the expression of *ASPARAGINE SYNTHETASE1* and *PROLINE DEHYDROGENASE2*. *Plant J.* 2008, *53*, 935–949.

[38] Weltmeier, F., Rahmani, F., Ehlert, A., Dietrich, K. et al., Expression patterns within the Arabidopsis C/S1 bZIP transcription factor network: availability of heterodimerization partners controls gene expression during stress response and development. *Plant Mol. Biol.* 2009, *69*, 107–119.

[39] Sambrook, J., Russell, D., David, W., *Molecular Cloning a Laboratory Manual*. Cold Spring Harbor Laboratory Press, NY, 1989.

[40] Bailey-Serres, J., Arabidopsis Cytoplasmic Ribosomal Protein Gene Family. 2004, http://www.arabidopsis.org/browse/genefamily/athr.jsp.

[41] Yamada, K., Lim, J., Dale, J. M., Chen, H. et al., Empirical analysis of transcriptional activity in the Arabidopsis genome. *Science* 2003, *302*, 842–846.

[42] Smyth, G. K., Linear models and empirical bayes methods for assessing differential expression in microarray experiments. *Stat. Appl. Genet. Mol. Biol.* 2004, *3*, Article3.

[43] Benjamini, Y., Hochberg, Y., Controlling the false discovery rate: a practical and powerful approach to multiple testing. *J. R. Stat. Soc. Series B* 1995, *57*, 289–300.

[44] Kawaguchi, R., Girke, T., Bray, E. A., Bailey-Serres, J., Differential mRNA translation contributes to gene regulation under non-stress and dehydration stress conditions in *Arabidopsis thaliana*. *Plant J.* 2004, *38*, 823–839.

[45] Muller, P. Y., Janovjak, H., Miserez, A. R., Dobbie, Z., Processing of gene expression data generated by quantitative real-time RT-PCR. *BioTechniques* 2002, *32*, 1372–4, 1376, 1378–9.

[46] Levin, Y., Hradetzky, E., Bahn, S., Quantification of proteins using data-independent analysis (MSE) in simple

andcomplex samples: a systematic evaluation. *Proteomics* 2011, *11*, 3273–3287.

[47] Geromanos, S. J., Vissers, J. P., Silva, J. C., Dorschel, C. A. et al., The detection, correlation, and comparison of peptide precursor and product ions from data independent LC-MS with data dependant LC-MS/MS. *Proteomics* 2009, *9*, 1683–1695.

[48] Li, G. Z., Vissers, J. P., Silva, J. C., Golick, D. et al., Database searching and accounting of multiplexed precursor and product ion spectra from the data independent analysis of simple and complex peptide mixtures. *Proteomics* 2009, *9*, 1696–1719.

[49] Eriksson, L., Antti, H., Gottfries, J., Holmes, E. et al., Using chemometrics for navigating in the large data sets of genomics, proteomics, and metabonomics (gpm). *Anal. Bioanal Chem.* 2004, *380*, 419–429.

[50] Tzafrir, I., Pena-Muralla, R., Dickerman, A., Berg, M. et al., Identification of genes required for embryo development in Arabidopsis. *Plant Physiol.* 2004, *135*, 1206–1220.

[51] Yao, Y., Ling, Q. H., Wang, H., Huang, H., Ribosomal proteins promote leaf adaxial identity. *Development* 2008, *135*, 1325–1334.

[52] Chen, J. G., Ullah, H., Temple, B., Liang, J. et al., RACK1 mediates multiple hormone responsiveness and developmental processes in Arabidopsis. *J. Exp. Bot.* 2006, *57*, 2697–2708.

[53] Guo, J., Wang, S., Wang, J., Huang, W. D. et al., Dissection of the relationship between RACK1 and heterotrimeric G-proteins in Arabidopsis. *Plant Cell Physiol.* 2009, *50*, 1681–1694.

[54] Nicolai, M., Roncato, M. A., Canoy, A. S., Rouquie, D. et al., Large-scale analysis of mRNA translation states during sucrose starvation in Arabidopsis cells identifies cell proliferation and chromatin structure as targets of translational control. *Plant Physiol.* 2006, *141*, 663–673.

[55] Chavez-Rios, R., Arias-Romero, L. E., Almaraz-Barrera Mde, J., Hernandez-Rivas, R. et al., L10 ribosomal protein from *Entamoeba histolytica* share structural and functional homologies with QM/Jif-1: proteins with extraribosomal functions. *Mol. Biochem. Parasitol.* 2003, *127*, 151–160.

[56] Warner, J. R., McIntosh, K. B., How common are extraribosomal functions of ribosomal proteins? *Mol. Cell* 2009, *34*, 3–11.

[57] Wool, I. G., Extraribosomal functions of ribosomal proteins. *Trends Biochem. Sci.* 1996, *21*, 164–165.

[58] Yacoub, A., Augeri, L., Kelley, M. R., Doetsch, P. W., Deutsch, W. A., A Drosophila ribosomal protein contains 8-oxoguanine and abasic site DNA repair activities. *EMBO J.* 1996, *15*, 2306–2312.

[59] Ferreyra, M. L. F., Pezza, A., Biarc, J., Burlingame, A. L., Casati, P., Plant L10 ribosomal proteins have different roles during development and translation under UV-B stress. *Plant Physiol.* 2010, *153*, 1878–1894.

[60] Wiese, A., Elzinga, N., Wobbes, B., Smeekens, S., A conserved upstream open reading frame mediates sucrose-induced repression of translation. *Plant Cell* 2004, *16*, 1717–1729.

[61] Wiese, A., Elzinga, N., Wobbes, B., Smeekens, S., Sucrose-induced translational repression of plant bZIP-type transcription factors. *Biochem. Soc. Trans.* 2005, *33*, 272–275.

[62] Sugihara, Y., Honda, H., Iida, T., Morinaga, T. et al., Proteomic analysis of rodent ribosomes revealed heterogeneity including ribosomal proteins L10-like, L22-like 1, and L39-like. *J. Proteome Res.* 2010, *9*, 1351–1366.

[63] Komili, S., Farny, N. G., Roth, F. P., Silver, P. A., Functional specificity among ribosomal proteins regulates gene expression. *Cell* 2007, *131*, 557–571.

[64] Weijers, D., Franke-van Dijk, M., Vencken, R. J., Quint, A. et al., An Arabidopsis minute-like phenotype caused by a semi-dominant mutation in a RIBOSOMAL PROTEIN S5 gene. *Development* 2001, *128*, 4289–4299.

[65] Xu, L., Xu, Y., Dong, A., Sun, Y. et al., Novel as1 and as2 defects in leaf adaxial-abaxial polarity reveal the requirement for ASYMMETRIC LEAVES1 and 2 and ERECTA functions in specifying leaf adaxial identity. *Development* 2003, *130*, 4097–4107.

[66] Byrne, M. E., Barley, R., Curtis, M., Arroyo, J. M. et al., ASYMMETRIC LEAVES1 mediates leaf patterning and stem cell function in Arabidopsis. *Nature* 2000, *408*, 967–971.

[67] Pinon, V., Etchells, J. P., Rossignol, P., Collier, S. A. et al., Three PIGGYBACK genes that specifically influence leaf patterning encode ribosomal proteins. *Development* 2008, *135*, 1315–1324.

[68] Vanlijsebettens, M., Vanderhaeghen, R., Deblock, M., Bauw, G. et al., An S18 ribosomal-protein gene copy at the Arabidopsis Pfl locus affects plant development by its specific expression in meristems. *EMBO J.* 1994, *13*, 3378–3388.

[69] Ito, T., Kim, G. T., Shinozaki, K., Disruption of an Arabidopsis cytoplasmic ribosomal protein S13-homologous gene by transposon-mediated mutagenesis causes aberrant growth and development. *Plant J.* 2000, *22*, 257–264.

[70] Rosado, A., Sohn, E. J., Drakakaki, G., Pan, S. Q. et al., Auxin-mediated ribosomal biogenesis regulates vacuolar trafficking in Arabidopsis. *Plant Cell* 2010, *22*, 143–158.

[71] Hirsch, C. A., Hiatt, H. H., Turnover of liver ribosomes in fed and in fasted rats. *J. Biol. Chem.* 1966, *241*, 5936–5940.

[72] Nikolov, E. N., Dineva, B. B., Dabeva, M. D., Nikolov, T. K., Turnover of ribosomal proteins in regenerating rat liver after partial hepatectomy. *Int. J. Biochem.* 1987, *19*, 159–163.

[73] Martin, N. C., Chiang, K. S., Goodenough, U. W., Turnover of chloroplast and cytoplasmic ribosomes during gametogenesis in *Chlamydomonas reinhardi*. *Dev. Biol.* 1976, *51*, 190–201.

[74] Baena-Gonzalez, E., Energy signaling in the regulation of gene expression during stress. *Mol. Plant* 2010, *3*, 300–313.

[75] Kawaguchi, R., Bailey-Serres, J., mRNA sequence features that contribute to translational regulation in Arabidopsis. *Nucleic Acids Res.* 2005, *33*, 955–965.

[76] Branco-Price, C., Kaiser, K. A., Jang, C. J. H., Larive, C. K., Bailey-Serres, J., Selective mRNA translation coordinates energetic and metabolic adjustments to cellular oxygen deprivation and reoxygenation in *Arabidopsis thaliana*. *Plant J.* 2008, *56*, 743–755.

[77] Piques, M., Schulze, W. X., Hohne, M., Usadel, B. et al., Ribosome and transcript copy numbers, polysome occupancy and enzyme dynamics in Arabidopsis. *Mol. Syst. Biol.* 2009, *5*, 1–17.

[78] Gibon, Y., Usadel, B., Blaesing, O. E., Kamlage, B. et al., Integration of metabolite with transcript and enzyme activity profiling during diurnal cycles in Arabidopsis rosettes. *Genome Biol.* 2006, *7*, R76.1–R76.23.

[79] Kawaguchi, R., Bailey-Serres, J., Regulation of translational initiation in plants. *Curr. Opin. Plant Biol.* 2002, *5*, 460–465.

[80] Branco-Price, C., Kawaguchi, R., Ferreira, R. B., Bailey-Serres, J., Genome-wide analysis of transcript abundance and translation in arabidopsis seedlings subjected to oxygen deprivation. *Ann. Bot.* 2005, *96*, 647–660.

[81] Wullschleger, S., Loewith, R., Hall, M. N., TOR signaling in growth and metabolism. *Cell* 2006, *124*, 471–484.

[82] Zinzalla, V., Stracka, D., Oppliger, W., Hall, M. N., Activation of mTORC2 by association with the ribosome. *Cell* 2011, *144*, 757–768.

[83] Ceci, M., Gaviraghi, C., Gorrini, C., Sala, L. A. et al., Release of eIF6 (p27BBP) from the 60S subunit allows 80S ribosome assembly. *Nature* 2003, *426*, 579–584.

